characterize the received signal. We will discuss statistical fading models for propagation effects in Chapter 3. Hybrid models, which combine ray tracing and statistical fading, can also be found in the literature [13; 14]; however, we will not describe them here.

The most general ray-tracing model includes all attenuated, diffracted, and scattered multipath components. This model uses all of the geometrical and dielectric properties of the objects surrounding the transmitter and receiver. Computer programs based on ray tracing – such as Lucent's Wireless Systems Engineering software (WiSE), Wireless Valley's SitePlanner®, and Marconi's Planet® *EV* – are widely used for system planning in both indoor and outdoor environments. In these programs, computer graphics are combined with aerial photographs (outdoor channels) or architectural drawings (indoor channels) to obtain a three-dimensional geometric picture of the environment [5].

The following sections describe several ray-tracing models of increasing complexity. We start with a simple two-ray model that predicts signal variation resulting from a ground reflection interfering with the LOS path. This model characterizes signal propagation in isolated areas with few reflectors, such as rural roads or highways. It is not typically a good model for indoor environments. We then present a ten-ray reflection model that predicts the variation of a signal propagating along a straight street or hallway. Finally, we describe a general model that predicts signal propagation for any propagation environment. The two-ray model requires information on antenna heights only; the ten-ray model requires antenna height and street/hallway width; and the general model requires these parameters as well as detailed information about the geometry and dielectric properties of the reflectors, diffractors, and scatterers in the environment.

### 2.4.1 Two-Ray Model

The two-ray model is used when a single ground reflection dominates the multipath effect, as illustrated in Figure 2.4. The received signal consists of two components: the LOS component or ray, which is just the transmitted signal propagating through free space, and a reflected component or ray, which is the transmitted signal reflected off the ground.

The received LOS ray is given by the free-space propagation loss formula (2.6). The reflected ray is shown in Figure 2.4 by the segments $x$ and $x'$. If we ignore the effect of surface wave attenuation[3] then, by superposition, the received signal for the two-ray model is

$$r_{\text{2-ray}}(t) = \text{Re}\left\{\frac{\lambda}{4\pi}\left[\frac{\sqrt{G_l}u(t)e^{-j2\pi l/\lambda}}{l} + \frac{R\sqrt{G_r}u(t-\tau)e^{-j2\pi(x+x')/\lambda}}{x+x'}\right]e^{j2\pi f_c t}\right\}, \quad (2.11)$$

where $\tau = (x + x' - l)/c$ is the time delay of the ground reflection relative to the LOS ray, $\sqrt{G_l} = \sqrt{G_a G_b}$ is the product of the transmit and receive antenna field radiation patterns in the LOS direction, $R$ is the ground reflection coefficient, and $\sqrt{G_r} = \sqrt{G_c G_d}$ is the product of the transmit and receive antenna field radiation patterns corresponding to the rays of length $x$ and $x'$, respectively. The *delay spread* of the two-ray model equals the delay between the LOS ray and the reflected ray: $(x + x' - l)/c$.

If the transmitted signal is narrowband relative to the delay spread ($\tau \ll B_u^{-1}$) then $u(t) \approx u(t-\tau)$. With this approximation, the received power of the two-ray model for narrowband transmission is

[3] This is a valid approximation for antennas located more than a few wavelengths from the ground.

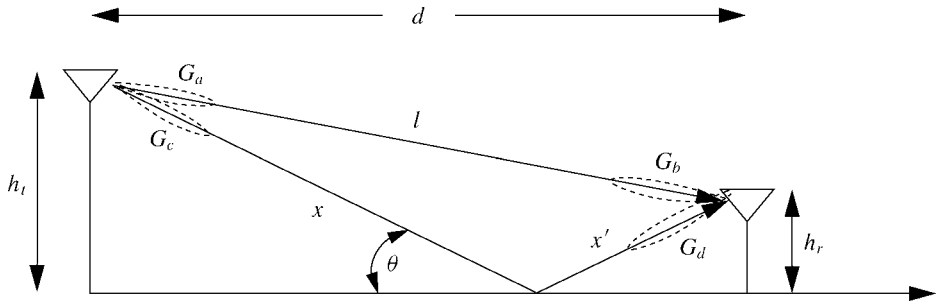


**Figure 2.4:** Two-ray model.

$$P_r = P_t\left[\frac{\lambda}{4\pi}\right]^2\left|\frac{\sqrt{G_l}}{l} + \frac{R\sqrt{G_r}e^{-j\Delta\phi}}{x+x'}\right|^2, \tag{2.12}$$

where $\Delta\phi = 2\pi(x + x' - l)/\lambda$ is the phase difference between the two received signal components. Equation (2.12) has been shown [15] to agree closely with empirical data. If $d$ denotes the horizontal separation of the antennas, $h_t$ the transmitter height, and $h_r$ the receiver height, then from geometry

$$x + x' - l = \sqrt{(h_t + h_r)^2 + d^2} - \sqrt{(h_t - h_r)^2 + d^2}. \tag{2.13}$$

When $d$ is very large compared to $h_t + h_r$, we can use a Taylor series approximation in (2.13) to get

$$\Delta\phi = \frac{2\pi(x + x' - l)}{\lambda} \approx \frac{4\pi h_t h_r}{\lambda d}. \tag{2.14}$$

The ground reflection coefficient is given by

$$R = \frac{\sin\theta - Z}{\sin\theta + Z}, \tag{2.15}$$

[6; 16], where

$$Z = \begin{cases} \sqrt{\varepsilon_r - \cos^2\theta}/\varepsilon_r & \text{for vertical polarization,} \\ \sqrt{\varepsilon_r - \cos^2\theta} & \text{for horizontal polarization,} \end{cases} \tag{2.16}$$

and $\varepsilon_r$ is the dielectric constant of the ground. For earth or road surfaces this dielectric constant is approximately that of a pure dielectric (for which $\varepsilon_r$ is real with a value of about 15).

We see from Figure 2.4 and (2.15) that, for asymptotically large $d$, $x + x' \approx l \approx d$, $\theta \approx 0$, $G_l \approx G_r$, and $R \approx -1$. Substituting these approximations into (2.12) yields that, in this asymptotic limit, the received signal power is approximately

$$P_r \approx \left[\frac{\lambda\sqrt{G_l}}{4\pi d}\right]^2\left[\frac{4\pi h_t h_r}{\lambda d}\right]^2 P_t = \left[\frac{\sqrt{G_l}h_t h_r}{d^2}\right]^2 P_t, \tag{2.17}$$

or, in dB,

$$P_r \text{ dBm} = P_t \text{ dBm} + 10\log_{10}(G_l) + 20\log_{10}(h_t h_r) - 40\log_{10}(d). \tag{2.18}$$

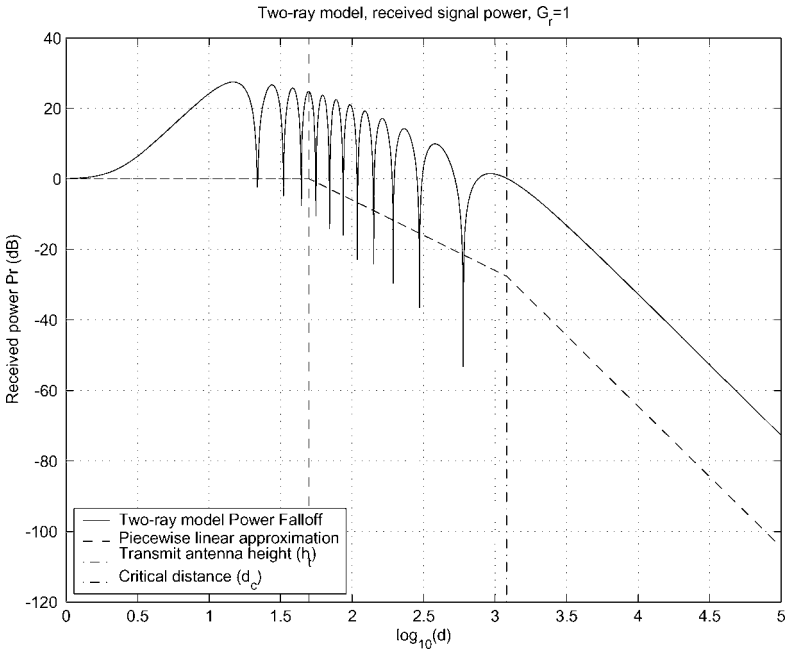


**Figure 2.5:** Received power versus distance for two-ray model.

Thus, in the limit of asymptotically large $d$, the received power falls off inversely with the fourth power of $d$ and is independent of the wavelength $\lambda$. The received signal becomes independent of $\lambda$ because directional antenna arrays have a received power that does not necessarily decrease with frequency, and combining the direct path and reflected signal effectively forms an antenna array. A plot of (2.12) as a function of distance is shown in Figure 2.5 for $f = 900$ MHz, $R = -1$, $h_t = 50$ m, $h_r = 2$ m, $G_l = 1$, $G_r = 1$, and transmit power normalized so that the plot starts at 0 dBm. This plot can be separated into three segments. For small distances ($d < h_t$) the two rays add constructively and the path loss is slowing increasing. More precisely, it is proportional to $1/(d^2 + h_t^2)$ since, at these small distances, the distance between the transmitter and receiver is $l = \sqrt{d^2 + (h_t - h_r)^2}$; thus $1/l^2 \approx 1/(d^2 + h_t^2)$ for $h_t \gg h_r$, which is typically the case. For distances greater than $h_t$ and up to a certain critical distance $d_c$, the wave experiences constructive and destructive interference of the two rays, resulting in a wave pattern with a sequence of maxima and minima. These maxima and minima are also referred to as small-scale or multipath fading, discussed in more detail in the next chapter. At the critical distance $d_c$ the final maximum is reached, after which the signal power falls off proportionally with $d^{-4}$. This rapid falloff with distance is due to the fact that, for $d > d_c$, the signal components only combine destructively and so are out of phase by at least $\pi$. An approximation for $d_c$ can be obtained by setting $\Delta\phi = \pi$ in (2.14), obtaining $d_c = 4h_t h_r/\lambda$, which is also shown in the figure. The power falloff with distance in the two-ray model can be approximated by averaging out its local maxima and minima. This results in a piecewise linear model with three segments, which is also shown in Figure 2.5 slightly offset from the actual power falloff curve for illustration purposes. In the first segment, power falloff is constant and proportional to $1/h_t^2$; for distances between

$h_t$ and $d_c$, power falls off at $-20$ dB/decade; and at distances greater than $d_c$, power falls off at $-40$ dB/decade.

The critical distance $d_c$ can be used for system design. For example, if propagation in a cellular system obeys the two-ray model then the critical distance would be a natural size for the cell radius, since the path loss associated with interference outside the cell would be much larger than path loss for desired signals inside the cell. However, setting the cell radius to $d_c$ could result in very large cells, as illustrated in Figure 2.5 and in the next example. Since smaller cells are more desirable – both to increase capacity and reduce transmit power – cell radii are typically much smaller than $d_c$. Thus, with a two-ray propagation model, power falloff within these relatively small cells goes as distance squared. Moreover, propagation in cellular systems rarely follows a two-ray model, since cancellation by reflected rays rarely occurs in all directions.

**EXAMPLE 2.2:** Determine the critical distance for the two-ray model in an urban microcell ($h_t = 10$ m, $h_r = 3$ m) and an indoor microcell ($h_t = 3$ m, $h_r = 2$ m) for $f_c = 2$ GHz.

**Solution:** $d_c = 4h_t h_r/\lambda = 800$ m for the urban microcell and 160 m for the indoor system. A cell radius of 800 m in an urban microcell system is a bit large: urban microcells today are on the order of 100 m to maintain large capacity. However, if we did use a cell size of 800 m under these system parameters, then signal power would fall off as $d^2$ inside the cell, while interference from neighboring cells would fall off as $d^4$ and thus would be greatly reduced. Similarly, 160 m is quite large for the cell radius of an indoor system, as there would typically be many walls the signal would have to penetrate for an indoor cell radius of that size. Hence an indoor system would typically have a smaller cell radius: on the order of 10–20 m.

### 2.4.2 Ten-Ray Model (Dielectric Canyon)

We now examine a model for urban microcells developed by Amitay [9]. This model assumes rectilinear streets[4] with buildings along both sides of the street as well as transmitter and receiver antenna heights that are close to street level. The building-lined streets act as a dielectric canyon to the propagating signal. Theoretically, an infinite number of rays can be reflected off the building fronts to arrive at the receiver; in addition, rays may also be back-reflected from buildings behind the transmitter or receiver. However, since some of the signal energy is dissipated with each reflection, signal paths corresponding to more than three reflections can generally be ignored. When the street layout is relatively straight, back reflections are usually negligible also. Experimental data show that a model of ten reflection rays closely approximates signal propagation through the dielectric canyon [9]. The ten rays incorporate all paths with one, two, or three reflections: specifically, there is the line-of-sight (LOS) path and also the ground-reflected ($GR$), single-wall ($SW$) reflected, double-wall ($DW$) reflected, triple-wall ($TW$) reflected, wall–ground ($WG$) reflected, and ground–wall ($GW$) reflected paths. There are two of each type of wall-reflected path, one for each side of the street. An overhead view of the ten-ray model is shown in Figure 2.6.

[4] A rectilinear city is flat and has linear streets that intersect at 90° angles, as in midtown Manhattan.

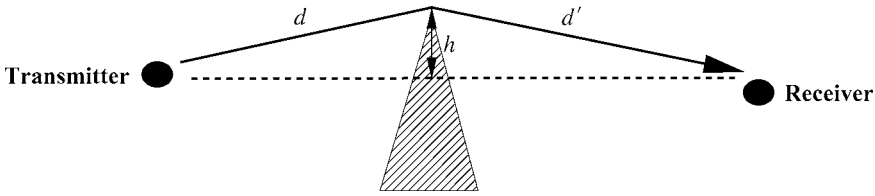


**Figure 2.7:** Knife-edge diffraction.

signal strength information for a particular transmitter and receiver configuration in a given environment.

The GRT method uses geometrical optics to trace the propagation of the LOS and reflected signal components as well as signal components from building diffraction and diffuse scattering. There is no limit to the number of multipath components at a given receiver location: the strength of each component is derived explicitly based on the building locations and dielectric properties. In general, the LOS and reflected paths provide the dominant components of the received signal, since diffraction and scattering losses are high. However, in regions close to scattering or diffracting surfaces – which may be blocked from the LOS and reflecting rays – these other multipath components may dominate.

The propagation model for the LOS and reflected paths was outlined in the previous section. Diffraction occurs when the transmitted signal "bends around" an object in its path to the receiver, as shown in Figure 2.7. Diffraction results from many phenomena, including the curved surface of the earth, hilly or irregular terrain, building edges, or obstructions blocking the LOS path between the transmitter and receiver [1; 5; 16]. Diffraction can be accurately characterized using the geometrical theory of diffraction (GTD) [25], but the complexity of this approach has precluded its use in wireless channel modeling. Wedge diffraction simplifies the GTD by assuming the diffracting object is a wedge rather than a more general shape. This model has been used to characterize the mechanism by which signals are diffracted around street corners, which can result in path loss exceeding 100 dB for some incident angles on the wedge [11; 24; 26; 27]. Although wedge diffraction simplifies the GTD, it still requires a numerical solution for path loss [25; 28] and thus is not commonly used. Diffraction is most commonly modeled by the *Fresnel knife-edge diffraction model* because of its simplicity. The geometry of this model is shown in Figure 2.7, where the diffracting object is assumed to be asymptotically thin, which is not generally the case for hills, rough terrain, or wedge diffractors. In particular, this model does not consider diffractor parameters such as polarization, conductivity, and surface roughness, which can lead to inaccuracies [26]. The diffracted signal of Figure 2.7 travels a distance $d + d'$, resulting in a phase shift of $\phi = 2\pi(d + d')/\lambda$. The geometry of Figure 2.7 indicates that, for $h$ small relative to $d$ and $d'$, the signal must travel an additional distance relative to the LOS path of approximately

$$\Delta d \approx \frac{h^2}{2}\frac{d + d'}{dd'};$$

the corresponding phase shift relative to the LOS path is approximately

$$\Delta\phi = \frac{2\pi\Delta d}{\lambda} \approx \frac{\pi}{2}v^2, \tag{2.21}$$

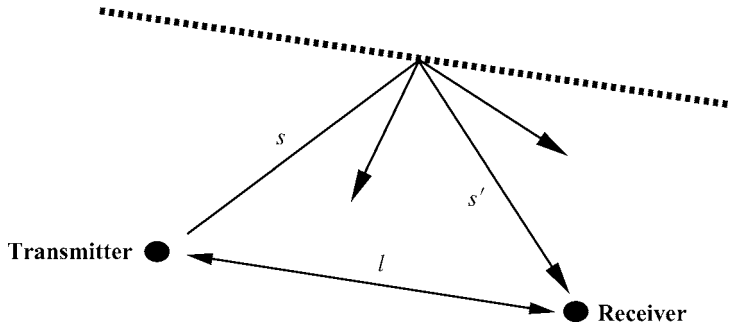


**Figure 2.8:** Scattering.

where

$$v = h\sqrt{\frac{2(d+d')}{\lambda dd'}} \tag{2.22}$$

is called the *Fresnel–Kirchhoff diffraction parameter.* The path loss associated with knife-edge diffraction is generally a function of $v$. However, computing this diffraction path loss is fairly complex, requiring the use of Huygens's principle, Fresnel zones, and the complex Fresnel integral [1]. Moreover, the resulting diffraction loss cannot generally be found in closed form. Approximations for knife-edge diffraction path loss (in dB) relative to LOS path loss are given by Lee [16, Chap. 2] as

$$L(v)\text{ dB} = \begin{cases} 20\log_{10}[.5 - .62v] & -0.8 \le v < 0, \\ 20\log_{10}[.5e^{-.95v}] & 0 \le v < 1, \\ 20\log_{10}\left[.4 - \sqrt{.1184 - (.38 - .1v)^2}\,\right] & 1 \le v \le 2.4, \\ 20\log_{10}[.225/v] & v > 2.4. \end{cases} \tag{2.23}$$

A similar approximation can be found in [29]. The knife-edge diffraction model yields the following formula for the received diffracted signal:

$$r(t) = \text{Re}\left\{L(v)\sqrt{G_d}u(t-\tau)e^{-j2\pi(d+d')/\lambda}e^{j2\pi f_c t}\right\}, \tag{2.24}$$

where $\sqrt{G_d}$ is the antenna gain and $\tau = \Delta d/c$ is the delay associated with the defracted ray relative to the LOS path.

In addition to diffracted rays, there may also be rays that are diffracted multiple times, or rays that are both reflected and diffracted. Models exist for including all possible permutations of reflection and diffraction [30]; however, the attenuation of the corresponding signal components is generally so large that these components are negligible relative to the noise. Diffraction models can also be specialized to a given environment. For example, a model for diffraction from rooftops and buildings in cellular systems was developed by Walfisch and Bertoni in [31].

A scattered ray, shown in Figure 2.8 by the segments $s$ and $s'$, has a path loss proportional to the product of $s$ and $s'$. This multiplicative dependence is due to the additional spreading loss that the ray experiences after scattering. The received signal due to a scattered ray is given by the bistatic radar equation [32]:

$$r(t) = \mathrm{Re}\left\{ u(t-\tau) \frac{\lambda \sqrt{G_s \sigma}\, e^{-j2\pi(s+s')/\lambda}}{(4\pi)^{3/2} s s'} e^{j2\pi f_c t} \right\}, \tag{2.25}$$

where $\tau = (s + s' - l)/c$ is the delay associated with the scattered ray; $\sigma$ (in square meters) is the radar cross-section of the scattering object, which depends on the roughness, size, and shape of the scatterer; and $\sqrt{G_s}$ is the antenna gain. The model assumes that the signal propagates from the transmitter to the scatterer based on free-space propagation and is then re-radiated by the scatterer with transmit power equal to $\sigma$ times the received power at the scatterer. From (2.25), the path loss associated with scattering is

$$\begin{aligned} P_r \text{ dBm} = {} & P_t \text{ dBm} + 10\log_{10}(G_s) + 20\log_{10}(\lambda) + 10\log_{10}(\sigma) \\ & - 30\log(4\pi) - 20\log_{10}(s) - 20\log_{10}(s'). \end{aligned} \tag{2.26}$$

Empirical values of $10\log_{10}\sigma$ were determined in [33] for different buildings in several cities. Results from this study indicate that $10\log_{10}\sigma$ in $\text{dBm}^2$ ranges from $-4.5\ \text{dBm}^2$ to $55.7\ \text{dBm}^2$, where $\text{dBm}^2$ denotes the dB value of the $\sigma$ measurement with respect to one square meter.

The received signal is determined from the superposition of all the components due to the multiple rays. Thus, if we have a LOS ray, $N_r$ reflected rays, $N_d$ diffracted rays, and $N_s$ diffusely scattered rays, the total received signal is

$$\begin{aligned} r_{\text{total}}(t) = \mathrm{Re}\Bigg\{ \Bigg[ \frac{\lambda}{4\pi} \Bigg] \Bigg[ & \frac{\sqrt{G_l}\, u(t) e^{j2\pi l/\lambda}}{l} + \sum_{i=1}^{N_r} \frac{R_{x_i} \sqrt{G_{x_i}}\, u(t-\tau_i) e^{-j2\pi x_i/\lambda}}{x_i} \\ & + \sum_{j=1}^{N_d} \frac{4\pi}{\lambda} L_j(v) \sqrt{G_{d_j}}\, u(t-\tau_j) e^{-j2\pi(d_j + d_j')/\lambda} \\ & + \sum_{k=1}^{N_s} \frac{\sqrt{G_{s_k}\sigma_k}\, u(t-\tau_k) e^{-j2\pi(s_k+s_k')/\lambda}}{\sqrt{4\pi}\, s_k s_k'} \Bigg] e^{j2\pi f_c t} \Bigg\}, \end{aligned} \tag{2.27}$$

where $\tau_i$, $\tau_j$, and $\tau_k$ are (respectively) the time delays of the given reflected, diffracted, and scattered rays – normalized to the delay of the LOS ray – as defined previously. The received power $P_r$ of $r_{\text{total}}(t)$ and the corresponding path loss $P_r/P_t$ are then obtained from (2.27).

Any of these multipath components may have an additional attenuation factor if its propagation path is blocked by buildings or other objects. In this case, the attenuation factor of the obstructing object multiplies the component's path-loss term in (2.27). This attenuation loss will vary widely, depending on the material and depth of the object [5; 34]. Models for random loss due to attenuation are described in Section 2.7.

### 2.4.4 Local Mean Received Power

The path loss computed from all ray-tracing models is associated with a fixed transmitter and receiver location. In addition, ray tracing can be used to compute the *local mean received power* $\bar{P}_r$ in the vicinity of a given receiver location by adding the squared magnitude of all the received rays. This has the effect of averaging out local spatial variations due to phase changes around the given location. Local mean received power is a good indicator of link quality and is often used in cellular system functions like power control and handoff [35].